Earth and Planetary Science Letters 308 (2011) 172–184

Contents lists available at ScienceDirect

Earth and Planetary Science Letters

journal homepage: www.elsevier.com/locate/epsl

Localised and distributed deformation in the lithosphere: Modelling the Dead Sea region in 3 dimensions

Maud Devès [a,*], Geoffrey C.P. King [a], Yann Klinger [a], Amotz Agnon [b]

[a] Institut de Physique du Globe, 1, rue Jussieu, Paris 75238, Cedex 05, France
[b] Institute of Earth Sciences, Hebrew University, Jerusalem, 91904, Israel

ARTICLE INFO

Article history:
Received 10 December 2010
Received in revised form 19 May 2011
Accepted 23 May 2011
Available online 12 June 2011

Editor: P. Shearer

Keywords:
Lithosphere mechanics, theory and modelling
Localised slip
Distributed deformation
Damage or process zone
Plate boundary strength
Fault system rheology

ABSTRACT

The Earth's lithosphere behaves as a strain softening elasto-plastic material. In the laboratory, such materials are known to deform in a brittle or a ductile manner depending on the applied geometric boundary conditions. In the lithosphere however, the importance of boundary conditions in controlling the deformation style has been largely ignored. Under general boundary conditions, both laboratory and field scale observations show that only part of the deformation can localise on through going faults while the rest must remain distributed in 'process zones' where spatially varying shear directions inhibit localisation. Conventional modelling methods (finite difference, finite or discrete elements) use rheologies deduced from laboratory experiments that are not constrained as a function of the geometry of the applied boundary conditions. In this paper, we propose an alternative modelling method that is based on the use of an appropriate distribution of dislocation sources to create the deformation field. This approach, because it does not rely on integrating differential equations from more or less well-constrained boundary conditions, does not require making assumptions on the parameters controlling the level and distribution of stresses within the lithosphere. It only supposes that strain accumulates linearly away from the dislocation singularities satisfying the compatibility equations. We verify that this model explains important and hitherto unexplained features of the topography of the Dead Sea region. Following the idea that strain can only localise under specific conditions as inferred from laboratory and field scale observations, we use our model of deformation to predict where deformation can localise and where it has to remain distributed. We find that ~65% of the deformation in the Dead Sea region can localise on kinematically stable through-going strike-slip faults while the remaining ~35% has to remain distributed. Observations suggest that distributed deformation occurs at stress levels that can be ten times greater than that associated with motion on well-localised faults. Thus, although only representing a minor part of the total deformation, distributed deformation should provide the greatest source of resistance to motion along this part of the Levant plate. These results can change dramatically our view of the behaviour of this and other plate boundaries. If the lithosphere can be regarded as a strain softening elasto-plastic material then similar behaviour should occur throughout, with important implications not only for its mechanical behaviour, but also for heat generation and related issues like metamorphism or magma genesis.

1. Introduction

In this paper we examine the implications of the continental lithosphere behaving as a strain softening elasto-plastic solid. While the existence of earthquakes on well-localised faults indicates that strain softening occurs in the upper crust, there is ample evidence that similar behaviour extends throughout the lower crust and mantle lithosphere. This includes geophysical observations of narrow faults or shear zones offsetting the Moho (e.g. Henstock et al., 1997; Wittlinger et al., 1998; Zhu, 2000), field observations of exhumed shear zones (e.g. Leloup and Kienast, 1993; Little et al., 2002) and highly sheared mantle-derived xenoliths along major shear zones (e.g. Titus et al., 2007). However, deformation in the lithosphere also demonstrably occurs in a distributed manner whether on innumerable small faults or fractures or in a more continuous fashion. De Sitter (1964) documents examples of distributed deformation throughout the crust.

The difficulty of building quantitative models has led to the emergence of several approaches with profoundly different assumptions. The lithosphere has been modelled as an assemblage of rigid blocks or as a viscous fluid responding to the boundary conditions dictated by plate tectonics. Models that assume rigid blocks have been easy to construct (Meade et al., 2002; Meade and Hager, 2005; Nyst and Thatcher, 2003). The fact that GPS vectors can be fitted within the

* Corresponding author.
E-mail address: deves@ipgp.fr (M. Devès).

0012-821X/$ – see front matter © 2011 Elsevier B.V. All rights reserved.
doi:10.1016/j.epsl.2011.05.044

measurement errors however mostly depends on a choice of block boundaries which sometimes bear little relation to geological observations and does not require that deformation indeed occurs by rigid blocks relative motion. Models based on numerical solutions of fluid flow equations that allow for spatially varying nonlinear viscosity have been adopted otherwise even major faults are not predicted. Molnar and Dayem, 2010 (and references therein) suggest that major strike-slip faults form at viscosity gradients in the mantle. However, these do not accord with observation. The Altyn Tagh fault for instance has propagated across major pre-Cambrian lithospheric structures (Meyer et al., 1998; Tapponnier et al., 2001).

The observation that major faults have evolved by propagation provides powerful evidence for the long-term strength of the continental lithosphere (e.g. Armijo et al., 1996, 2003; Flerit et al., 2003, 2004; Hubert-Ferrari et al., 2003). Materials that retain long term strength and experience strain localisation have been modelled considering localisation to be entirely controlled by stress conditions. In this approach, localisation starts and develops where stresses are higher than a given yield stress (e.g. Regenaeur-Lieb et al., 2008). A major problem with this approach is the difficulty of defining and computing models with realistic boundary conditions. Modelling realistic 3 dimensional structures is almost impossible. A further problem is determining the appropriate stress conditions for localisation when even at the laboratory scale, the onset of irreversible deformation (or plasticity) can vary with boundary conditions and is thus not a readily defined material property. An important objective of this approach is to predict the appearance and growth of faults, but for Earth problems this seems complicated and to some extent unnecessary. The dimensions and offsets or deformation rates of important faults are known a priori from geological data rendering it more reasonable to regard them as “knowns” rather than seek them as “unknowns”.

Models based on analogue experiments with sand or other materials have also been extensively used and this approach has provided insight (e.g. Peltzer and Tapponnier, 1988; Wu et al., 2009). Although they can incorporate aspects of the behaviour of elasto-plastic materials and features that are inherently 3 dimensional, laboratory conditions do not allow all reasonable boundary conditions to be tested. Moreover, the analogue materials have scale dependent rheologies making the results difficult to extrapolate to the scale of the lithosphere.

All of the foregoing methods are time consuming taking many hours for each simulation. While having limitations, the models we create take less than a minute to compute allowing many to be tested. The reasons for adopting more time consuming techniques should be seriously questioned. Our approach does not depend on integrating from an assumption of small-scale rheology to predict large-scale behaviour. We create a 3D kinematic model of the deformation field. Except at such boundaries the material is assumed to deform in a linear fashion. The validity of the linear approximation can be tested directly by comparing the predicted deformation with geological and geomorphological observations. We then use simple criteria based on both laboratory and field scale observations to determine where deformation can localise and where it must remain distributed. Conveniently the use of dislocations allows us to quantify how much of the deformation is localised and how much is distributed. Combined with independent observations on the difference of stresses involved in localised and distributed deformation, it eventually allows us to provide an estimate of the stress distribution without having made assumptions either on the rheology or on the initial stress field.

We illustrate this approach by examining the mechanics of the Dead Sea region (Jordan and Araba valleys) of the Levant. A kinematic model of the deformation field is created by distributing dislocations in an infinite medium outside the region we wish to model. The deformation field is chosen such that it reproduces the overall morphological features of the region. Having found a suitable deformation field we then determine where deformation can localise on large faults and where it must remain distributed and explore the implications for stress distribution within the lithosphere and at plate boundaries.

2. Localised and distributed deformation

Features characteristic of deformation in a strain softening elasto-plastic material are perfectly illustrated by the well-known plasticine indentor experiments (Peltzer and Tapponnier, 1988). An example is shown in Fig. 1. Plasticine behaves in an elasto-plastic manner and has strain-softening properties. After a given amount of displacement has been applied at the sample's boundaries, faulting appears, but not everywhere. Faults first appear in regions of low strain where, once initiated by some tiny defect, a fault can extend. To do so the fault must follow simple shear directions, which extend in a straight line or a simple arc over some distance. Such faults are kinematically stable meaning that their strain environment permits them to acquire substantial displacement without changing geometry. In other regions, kinematically stable faults cannot develop even if the strain is high. In these regions a fault can initiate but can only extend over a small distance because simple shear directions change from place to place. In these regions deformation accumulates in a distributed manner. This can either be by creating many small faults with various orientations that never accumulate large displacements, or in the form of continuum deformation where individual faults cannot be discerned. Although there is limited information concerning the strength of elasto-plastic materials for different failure modes, localised deformation seems to occur more readily than distributed deformation.

Fig. 2 explains schematically how boundary conditions can determine the deformation style for a strain-softening medium. Fig. 2a shows the deformation field (shown as flow lines for visualisation) in a linear material subject to simple shear boundary conditions. Only one component of shear is applied and the resulting deformation field is independent of position. Fig. 2b shows that in a strain-softening material, the same boundary conditions can be

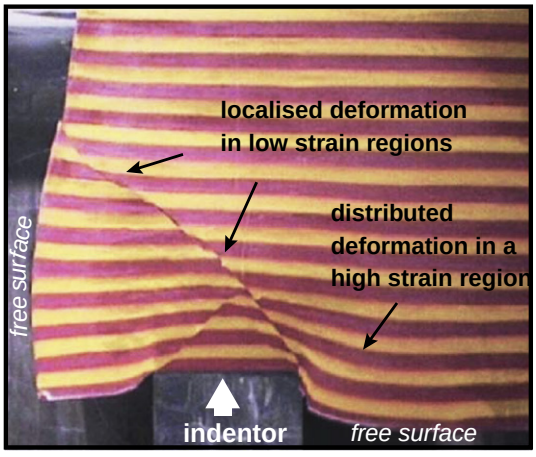

Fig. 1. Plasticine experiment adapted from Peltzer and Tapponnier (1988). During indentation, two stable faults form following simple shear directions as predicted by the slip line theory. It is interesting to observe that no faults appear in some regions undergoing high strain. There, strain cannot localise and accumulates in a distributed manner. This experiment illustrates well the complementary role played by localised and distributed deformation in releasing an applied strain and underlines the importance of the kinematics and geometry of the boundary conditions in controlling their interrelationship. McClintock (1971) had already emphasised this particular behaviour of elasto-plastic materials but to our knowledge there are still today no empirical or analytical laws describing it.

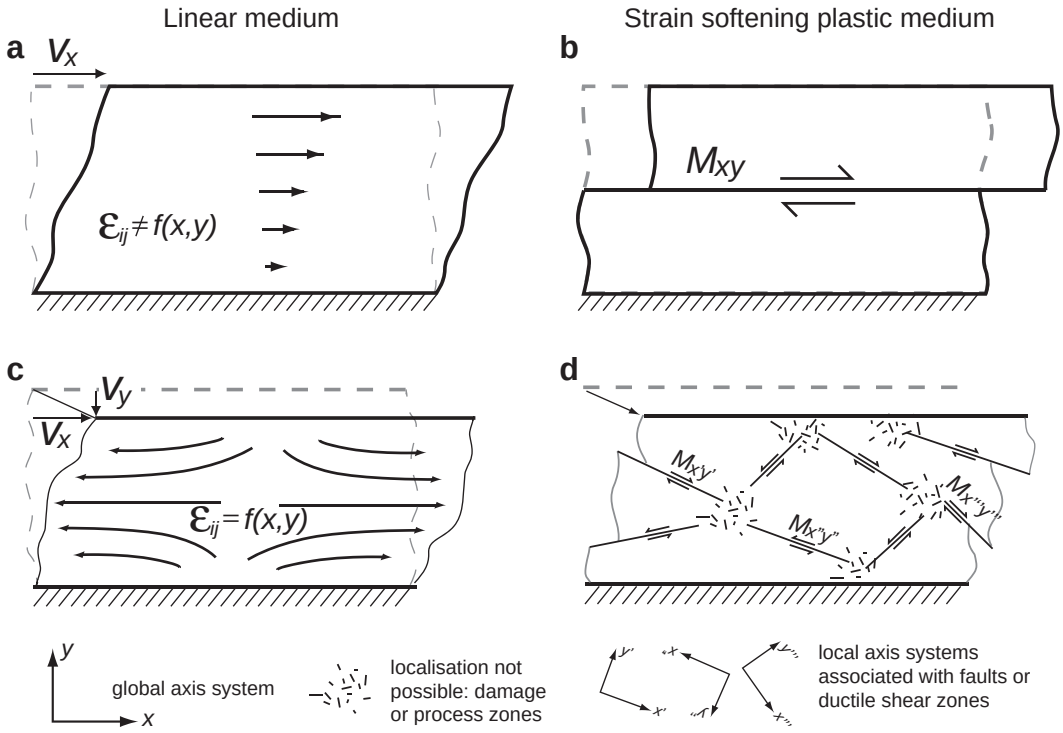

Fig. 2. Deformation in strain softening plastic materials. a) Shows a displacement distribution in a linear material subject to simple shear boundary conditions. The strain field, which has a single shear component, is independent of position. b) For the same boundary conditions, a single localised feature, a fault or a shear zone, can completely relieve the applied displacement. Note that this fault has formed along a line of maximum shear strain. c) Shows displacements in a linear viscous material with more common boundary conditions. Strain is a function of position and is not composed of a single shear component. d) In a strain softening plastic material, most of the deformation can be accommodated by localised slip on faults with various orientations. However, there are kinematic incompatibilities where these faults meet. This results in zones of distributed deformation that can be referred to as 'process zones' or 'damage zones' where strain cannot localise (cf. explanation Fig. 3). We see that distributed and localised deformations are both required in order to release the applied boundary conditions and that the two deformation styles are intrinsically related. Their relative distribution is controlled first by the kinematics and geometry of the applied boundary conditions and second by the kinematics and geometry of the system of faults that has developed in response to these boundary conditions.

accommodated by localisation on a single feature (fault or shear zone). The boundary conditions in Fig. 2c are more common. The induced deformation has more than one component and is a function of position. Fig. 2d shows schematically that in a strain-softening medium, it is no longer possible to relieve the boundary conditions on a single localised feature. Faults of different orientations develop following simple shear directions but motion along them cannot accommodate all the strain. In the regions where faults with different orientations meet, the deformation field is locally affected by the geometry and kinematics of the various faults. Zones of complicated deformation field are created where simple shear directions cannot be collinear preventing localisation to occur over long distances. The most basic form of fault interaction in two dimensions is a triple junction (Morgan and McKenzie, 1969). Fig. 3 illustrates the case of a junction between three strike-slip faults. Such a junction is kinematically unstable. Motion on the main faults must be accommodated at the junction either by a volume change (Fig. 3a) or by inelastic deformation off the main faults (Fig. 3b, c, d). In the lithosphere, confining pressure prevents opening of large voids or overlapping of material and thus inelastic deformation must accumulate off the main faults in zones where, as shown in Fig. 3c and d, simple shear directions are not collinear over long distances preventing localization. Such zones accommodate large strains by distributed deformation and can be referred to as 'damage zones', or 'process zones'. In brittle materials, 'process zones' of distributed deformation can be composed of a self-similar (fractal) complex of faults that continuously require fracture of new material (see Figure S5 in Supplementary Material) (King, 1983; King, 1986).

Laboratory experiments in rocks to reproduce the features shown in Fig. 2d are difficult to mount. Fully triaxial tests on rocks show that multi-directional faulting is created (e.g. Reches, 1983; Reches and Dieterich, 1983) but only very small displacements can be applied before the sample breaks apart – too small for process zones to be (clearly) observed. Applying significant displacements for complex boundary conditions while keeping the sample confined to prevent fragmentation has not been successfully achieved. This is one reason why materials such as sand, clay or plasticine are favoured for laboratory experiments. They can localise at one scale but distribute deformation at smaller scales and hence do not fragment. However, this convenient scale dependent behaviour means that they can only provide limited insight into how the lithosphere behaves.

Structural geologists have long appreciated that folding occurs by distributed deformation either brittle (e.g. Suppe, 1984) or ductile associated with faulting. King and Brewer (1983) document an example of folding at seismogenic depths associated with the Wind River thrust. Other examples can be found in De Sitter (1964) or King and Yielding (1984). Process zones are more familiar to engineers when referring to crack tip process in Linear Elastic Fracture Mechanics (LEFM). The term 'process zone' has been used to describe deformation associated with propagating faults (Armijo et al., 2003, Cowie and Scholz, 1992, Flerit et al., 2004, Manighetti et al., 2004). In these cases they form a transitory region of complex deformation that appears prior to the propagation of a fault into a previously unfractured material. Once the fault end has propagated past, the old process zone becomes inactive. Although not generally described as such in the past, process zones also form at complexities such as bends or offsets in fault systems where, while the main fault geometries are maintained they are permanent features where damage evolves with each increment of slip on the main faults (King, 1983). These long-lived process zones are recognised to play a

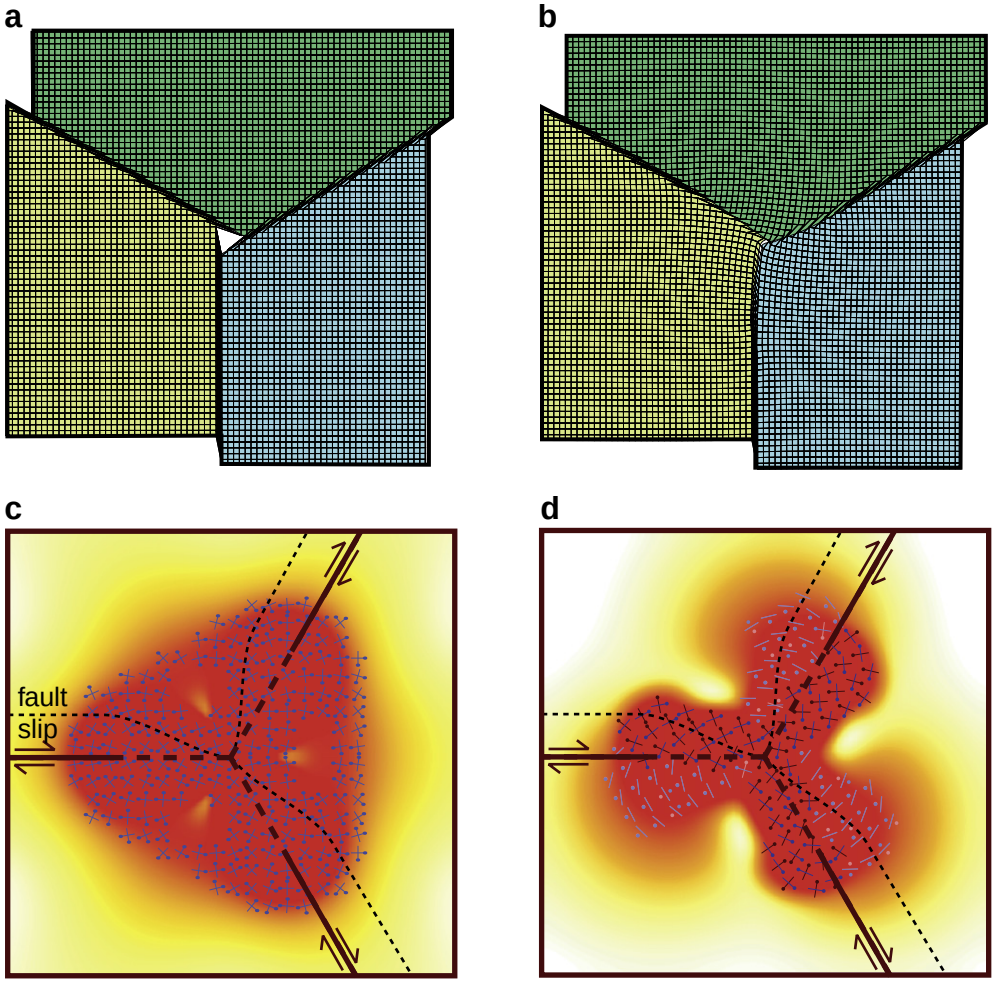

Fig. 3. Junctions between strike-slip faults are kinematically unstable (Morgan and McKenzie, 1969). They are however observed at the Earth's surface (e.g. junctions between the North and East Anatolian faults in Turkey). The deformation associated with such junctions can be accommodated in two ways. a) It can be accommodated by a volume change. A void opens as finite motion accrued on the main faults separating three undeforming blocks. b) It can be accommodated by distributed deformation off the main faults. In the Earth's lithosphere, confining pressure prevents large volume changes and deformation accumulates off the main faults in a distributed manner in order to respect the condition of zero slip at the junction. c) The shear strain (in red see caption Fig.7) induced off faults around the junction is shown for a plane strain model (2D). Dashed curves illustrate the slip distribution on the main faults. Slip comes to zero at the junction between the three faults. Symbols represent the predicted slip directions (see caption Fig. 7). Whereas mechanisms are all strike-slip, they change directions from place to place preventing localisation to occur on long distances. Deformation can only be accommodated in a distributed manner, which can occur for instance by motion on many small faults (or shear zones) with different directions or in a more continuous fashion. d) The shear strain (in red) induced off faults around the junction is shown for a plane stress model with a compressional out of plane principle strain. The strain distribution is changed and some mechanisms are normal faulting but again deformation has to remain distributed, localisation cannot develop on long distances because of highly variable slip directions.

key role in the seismic behaviour of fault systems (King, 1986; King and Nabelek, 1985; Klinger, 2010; Klinger et al., 2006). At the scale of the tectonic plates, process zones should be found at any junctions between plate boundaries that are kinematically incompatible. The junction between the North and East Anatolian faults in Turkey for instance cannot be stable over time (Hubert-Ferrari et al., 2009). It has however been maintained over at least the last three million years thanks to the accommodation of deformation off the main faults. The development of process zones of distributed deformation can help to stabilise incompatible junctions but they can evolve in due course.

3. Modelling using dislocations

An alternative approach to solving the equilibrium and compatibility equations by integration from applied boundary conditions is using a distribution of strain sources representing displacement discontinuities to produce the required deformation in a specified region. Many problems in solid mechanics can be solved using an array of dislocations. Dislocations can be described as Somigliana or Volterra (Nabarro, 1967, Eshelby, 1973). In the former, the dislocation is a surface on which the displacement discontinuity is defined by a grid of points. In the second, the dislocation is a line along which the displacement discontinuity is constant. While the two representations are equivalent, they have different practical applications (Eshelby, 1973). Seismologists commonly use Somigliana dislocations to represent slip on a fault plane, while those studying crystal deformation use Volterra dislocations to describe the displacement of a line of atoms. In each case, three modes describe two directions of in-plane slip and one of opening. A combination of Volterra dislocations can be used to reproduce a Somigliana one. A line dislocation (Volterra) has a certain angle with respect to the slip direction. A portion of dislocation where the dislocation line direction is perpendicular to slip is called an edge dislocation. If it is parallel to the slip direction, it is called a screw dislocation. A Volterra dislocation with more general orientation is called a mixed dislocation.

Problems solved using dislocations obey the compatibility equations. Thus provided the gradient of displacement remains large compared to its squares (roughly that the squares of strains are small

compared to strains), the resulting deformation field has an analytic solution. Although commonly referred to as an elastic solution Jaeger et al. (2007) (p 106) point out that it provides a close approximation for many problems that involve permanent deformation. As Nabarro (1967) says "The idea of dislocation is essentially geometrical" and using a distribution of dislocations to model deformation in a given region is an approach that is essentially kinematic. Poisson's ratio is the only material parameter required because the problems are specified in terms of displacements and not in term of stresses. The technique hence remains valid when substantial deformation occurs and is not limited to infinitesimal deformation.

A similar approach can be taken to numerically solve general problems by the use of dislocations (e.g. Crouch and Starfield, 1983). It is important to emphasise that provided the deformation field in the region we study is correct, it is not important to know how this is achieved. A common example of this approach is the use of image and other dislocations to create analytic expressions for a rectangular plane of slip in a half space (e.g. Jaeger et al., 2007; Okada, 1985). The only significance of the image dislocations is that they produce a surface that is stress free at the appropriate place in the infinite medium. The part of the medium containing the image sources is disregarded. Although expressions for dislocations in a half space are analytic they are complicated and producing a debugged computer code is time consuming. Okada (1985) however developed a reliable kinematic code, which describes rectangular dislocations with uniform slip in a linear half-space. We adopt Okada's code to provide a stress free ground surface and we do not show image sources explicitly. In our application, we refer to rectangular Somigliana dislocations as "elements" and to their Volterra boundaries as "dislocations". Deformation predicted outside the region is ignored. We do not need all of the dislocations that are included to define a rectangular area. The unnecessary ones can be ignored by placing them at (approximately) infinite distance.

Fig. 4 shows the basis of the modelling in cross-section. In Fig. 4a, a rectangular dislocation extends from 15 km to infinite depth. There are three directions of slip: two directions of in-plane slip and one of opening. Relative displacement in the y–z plane is shown by arrows. An out of plane displacement is applied in the x-direction. Using a rectangular dislocation is equivalent to bounding the area of this dislocation with line dislocations as shown in Fig. 4b. The line direction of these dislocations is perpendicular to the slip direction. They are called edge dislocations. Since the deformation associated with a dislocation decays with distance it is clear that dislocations at an infinite distance from the modelled region can be ignored. Only the mixed dislocation at a depth of 15 km determines the deformation field in the modelled region. At a distance from the region the medium moves as two undeformed blocks. This is considered to be the plate motion and need not be specified in any other way. Provided the

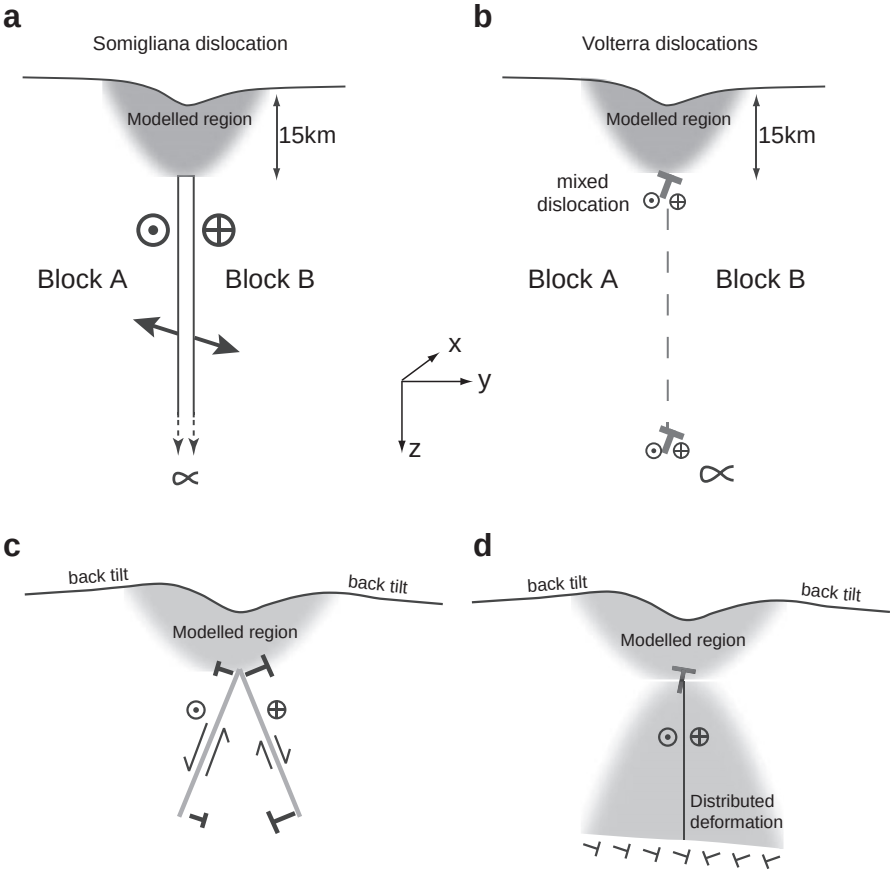

Fig. 4. Modelling deformation in a region using dislocations. a) The deformation is represented as being modelled using a Somigliana dislocation extending from a depth of 15 km to infinite depth. The dislocation has a constant offset in the y, z directions. The model can also be specified in the x direction assumed to be plus and minus infinity for this figure. The results of Okada (1985) can model this geometry. b) The deformation is represented as being modelled using Volterra dislocations. Two line dislocations one at a depth of 15 km and one at infinite depth are shown. Two vertical line dislocations lie outside the plane in the x direction at plus and minus infinity. The dislocations include edge and screw components with Burgers vectors to give the appropriate deformation. c) A single edge dislocation can be decomposed into two or more dislocations. The same deformation field could result from two antithetic faults defined by four edge dislocations: two at the surface and two at a finite depth. The latter result in some long wavelength deformation in the modelled region. d) The two lower dislocations could be distributed to represent a zone of distributed deformation that can be cut by a strike slip fault. Again this dislocation distribution results in some long wavelength deformation in the modelled region.

deformation in the modelled region is satisfactory (in the following, this will be done by comparing the vertical component of the modelled deformation field with surface topography) it is not necessary to provide a physical explanation for what the dislocations could represent, however some guide is provided in Fig. 4c and d. An edge dislocation can be separated into two dislocations, such as illustrated in Fig. 4c, and the deformation field could result from two antithetic faults. The upper dislocations at a depth of 15 km dominate the deformation in the modelled region. If the lower dislocations are at infinite depth, the deformation in the modelled region remains identical to that for an equivalent single edge dislocation. If they are brought closer to the surface some long-wavelength deformation can become superimposed on deformation in the modelled region due to the upper dislocation (Fig. 4d). Models of this sort (e.g. Armijo et al., 1996; Stein et al., 1988) result in a small back tilt as indicated in the Fig. 4c and d. Deformation at depth could alternatively be distributed, as illustrated in Fig. 4d. But again, this would not affect significantly the deformation in the modelled region.

4. The Dead Sea region

Choosing a 'right' natural example to illustrate the distribution between distributed and localised deformation within the lithosphere and explore the role of the kinematics and geometry of the boundary conditions is not straightforward. Choosing the 'right' scale to address the issue is difficult. It seemed reasonable for us to focus our study at the scale of a 'relatively simple' plate boundary, that of the Levant. We have chosen a window extending for a few hundred kilometres distant from the plate boundary extremities where the interaction with other plate boundaries complicates the scheme. The region of the Dead Sea is of particular interest because although most agree that the Dead Sea valleys are tectonic in origin, no one agrees on the processes that have led to its formation. There has been a wide range of interpretations and changing views of the history of valley opening, which have not always been consistent (see Supplementary material).

Fig. 5 shows a south looking 3D view of the Dead Sea region with a satellite image (Fig. 5a) and colour coded topography (Fig. 5b) draped on the topography. There are two striking features. First, the two valleys average more than 600 m in depth. Second there is an ~11.5° change of direction between them. The form of the two valleys is similar. However, the valley floor is below sea level in the north and partly above sea level in the south. Fig. 5a shows mapped active faults between Lebanon in the north to the Gulf of Aqaba in the south where they are unambiguous. With the exception of the Carmel fault, these are predominantly strike-slip. Although it has been suggested that the Carmel fault has a substantial component of strike-slip it has the classic features of simple normal faulting: a single dipping and eroded escarpment with the hanging wall down-warped and the footwall up-warped. Long-term motion on this fault has created the present day topography (see other examples in Armijo et al., 2003 and Stein et al., 1988). An intriguing observation is that there are no simple large normal faults running along the valley's flank that could account for its formation. The most prominent normal fault within the valleys is the east–west Amaziahu fault (~50 m of vertical offset), which is a clear feature, local to the Dead Sea itself and roughly perpendicular to the trend of the main valleys. A close examination of the valleys using Google Earth perhaps reveals a few possible normal faults associated with the valley flanks (e.g. Amit et al., 2002; Garfunkel et al., 1981;

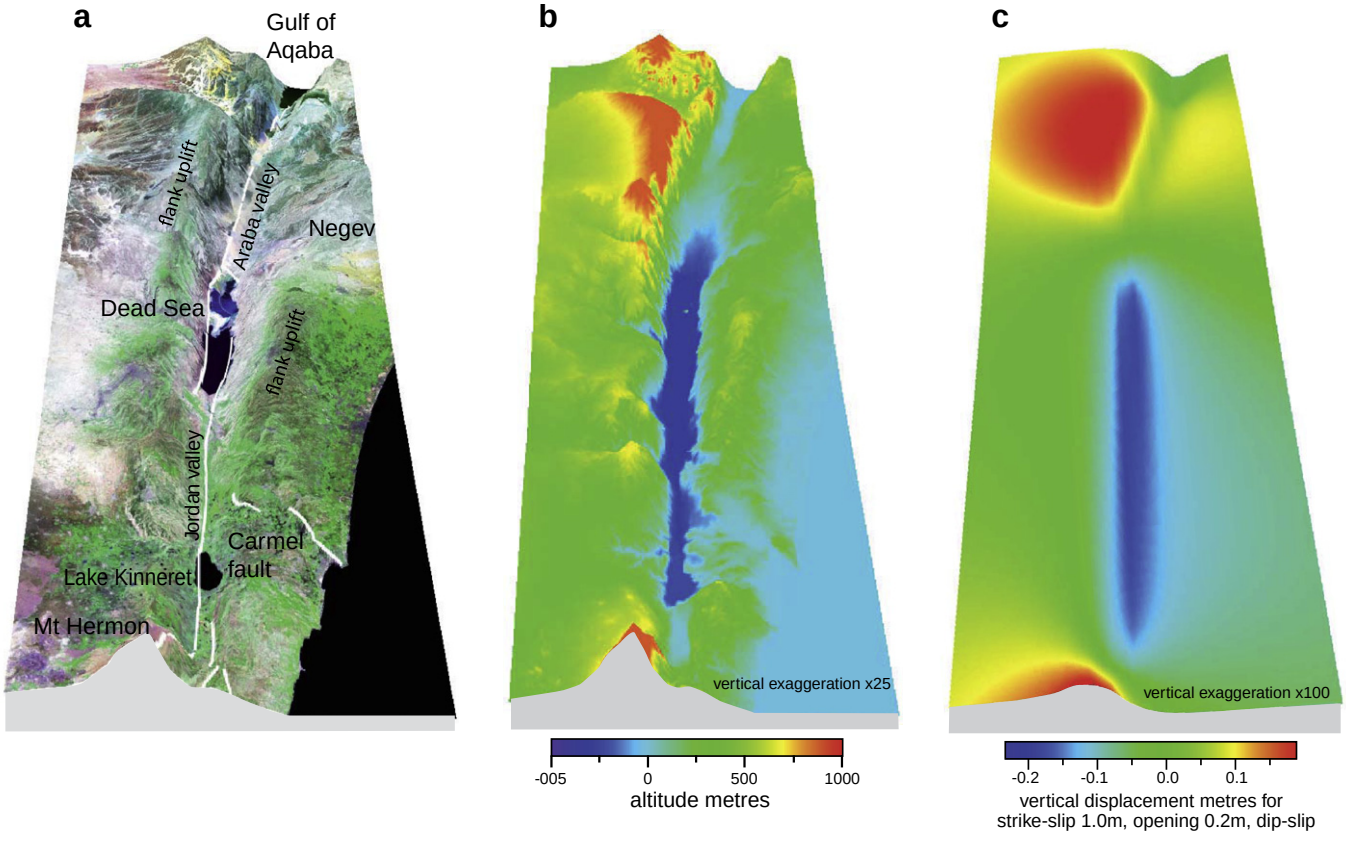

Fig. 5. Topographic representations of the Dead Sea valleys. a) Shows a Landsat thematic mapper image (band 2-red, 4-green, and 7-blue) draped over exaggerated digital elevation data (SRTM 3) to give a 3D effect. The vertical exaggeration is 25. The most prominent feature is the 11.5° change of valley strike occurring at the Dead Sea. While the valley is a clear feature there are no clear normal faults along the valley flanks (unlike Carmel fault) such as in true rifts like Corinth or East Africa. b) Shows a 3D image of the topography (SRTM3 data) coloured by altitude. c) Shows uplift and subsidence rates predicted by the model.

Klinger et al., 2000). However they are notable by their modest length, small throw and insignificance compared to the greater than 600 m of offset between the valley floor and flanks. The immediate region of the Dead Sea has been explained mechanically as a pull-apart (Garfunkel, 1981) with less attention being paid to the role of the change in strike, which can be thought of as producing a releasing bend. Whatever the mechanical processes it is locally a very deep trough both filled and masked by sediments making it difficult to study the kinematics in any detail.

In the following, we concentrate on the large scale features of deformation in the region and explore whether they can be explained by a combination of localised and distributed deformation on the basis of simple kinematical assumptions.

5. Modelling the Dead Sea region

The features of the deformation in the Dead Sea region are associated with opening, strike-slip motion and possibly relative uplift of the eastern sides of the valleys relative to their western side. Two rectangular elements characterise most of the valley (Fig. 6a). The elements extend from 15 km to 5000 km. Details of the elements are shown in the Supplementary material. Fig. 6b, c and d use a two-element

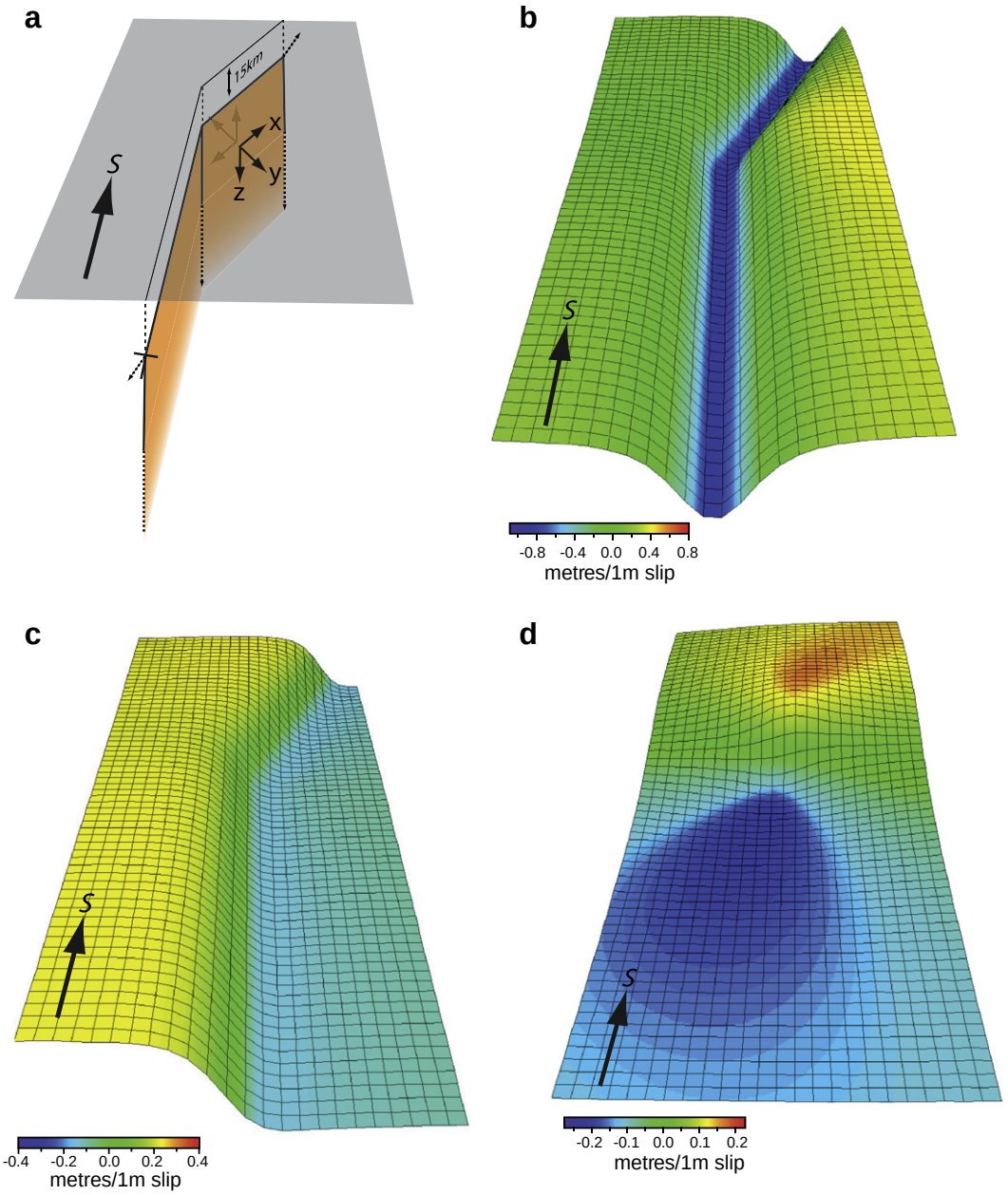

Fig. 6. Deformation is modelled using dislocations. a) Rectangular elements lie beneath the axis of the valley at a depth of 15 km and extend to a depth of 5000 km (~infinity). Two elements are used to characterise most of the valley, but to avoid end effects, elements extend to the north into Lebanon and Syria and south into the Gulf of Aqaba and the Red Sea (see Supplementary Material). b) c) and d) show surface uplift and subsidence for a simplified model that includes the elements drawn in a) but extending to a very large distance outside the region plotted. b) Shows the surface displacement due to opening (y-direction). c) Shows the surface displacement due to dip-slip motion (z-direction). d) Shows uplift and subsidence that results from the change of strike of the strike-slip motion. Horizontal motion due to strike-slip motion (x-direction) is not shown. It is this uplift and subsidence that causes the Jordan valley to be below sea level and the Araba valley above sea level.

model (Fig. 6a) to show respectively the vertical displacements at the surface due to opening, dip-slip and strike-slip motion. Adjusting their contributions provides the major features of the deformation in the modelled region. This two-dislocations model could of course be refined in order to model second order features of deformation within the valleys. For proof of concept however, we settle for using the simplest model possible. We add further elements to model the north end of the Gulf of Aqaba and Mount Hermon and avoid the large strains that would result from abruptly terminating the model, but for simplicity are not included in Fig. 6. Opening creates the overall distributed deformation that forms the valleys (Fig. 6b). Dip slip causes the eastern flank to be uplifted relative to the western flank (Fig. 6c). Fig. 6d shows that the change of strike of the strike-slip motion results in distributed uplift to the south and distributed subsidence to the north (discussed by Bilham and King, 1989). To our knowledge this important effect is not included in any other modelling of the Dead Sea valleys' system.

Fig. 5c shows uplift and subsidence for the complete model with 1 m of strike-slip. The best prediction is obtained when both valleys are assigned 0.2 m of opening and 0.03 m of dip-slip. The topography predicted in Fig. 5c can be compared with the present day topography shown in Fig. 5b. A similar rainbow colour scheme is used to represent altitude. The broad topography correlates well with uplifted and subsided regions. Our approach provides a view of the deformation that is not time-dependent and can hence accommodate varying assumptions about timing. It is widely accepted that the Dead Sea fault system was initiated about 15 Ma ago. Local sediment formations show however that the transform margins were not much uplifted until 10 Ma ago (see Garfunkel, 1997 for a review). Although a consensus accepts a 107 km of horizontal offset for the southern part of the Dead Sea fault (the region addressed in this paper), definitive timing remains uncertain. Of this offset, only 40–45 km appears to be of post-Miocene age (e.g. Freund et al., 1968). With the ratio of strike-slip to opening used in Fig. 5c and for a strike-slip component lying between 5 and 10 mm/year, the predicted average opening rate lies between 5 and 10 mm/year over that period. These values are reasonable given the limited geological evidence (Supplementary material). The mechanical discussion that follows remains valid provided that some strike-slip and opening have acted together.

6. Identifying regions of localised and distributed deformation

The approach we adopt is similar to that used to explain slip partitioning by upward propagation of deformation (Bowman et al., 2003; King et al., 2005). In these papers, kinematically stable faults were considered to form where predicted fault directions allowed a fault to initiate and, once created, to extend and accommodate a substantial part of the applied deformation field. As noted earlier, for faults to fully relieve the boundary conditions (see caption to Fig. 2), they must follow simple shear directions.

Fig. 7a shows the fault mechanisms predicted at the surface for the same model as Fig. 5c. White lines indicate currently active faults with strike-slip faults predominating. The interpretation of the symbols indicating the mechanisms is shown in Fig. 7b. It can be seen that within the valley, strike-slip mechanisms predominate and are co-linear fulfilling the kinematic requirement for the creation of stable faulting. At the edges and flanks of the valley, normal and oblique faulting is predicted, but in highly variable directions. Fig. 7c shows a schematic cross-section and indicates the location of the three depth sections shown in Fig. 7d. These show that while strike-slip faulting is predicted at all depths beneath the valley, the mechanisms predicted beneath the flanks changes with depth. Thus strike-slip faults can become stable both laterally and with depth, but dip-slip and oblique faultings can do neither and require the creation of further faulting with various orientations to accommodate the deformation. The multiple and multi-scale faulting associated with these regions must continuously evolve to form a process zone. Such multi-direction faulting has been mapped along parts of the valley flanks by Sagy et al. (2003) and has been related to the work of Reches and Dieterich (1983) and Reches (1983) discussed earlier. Large valley parallel normal faults are not predicted. The calculation to create Fig. 7 adds a regional extensional strain field. As in Coulomb stress interaction calculations (review King, 2007), it ensures that most of the predicted mechanisms are consistent with the direction of the horizontal principal axis determined from seismic data by Hofstetter et al., 2007. In the Supplementary material, we show two alternative regional strain conditions. Fig. S4a shows the result with no added regional strain field and Fig. S4b for a small vertical contraction. For the regions of high strain the predicted style of faulting is almost identical. Outside the region the mechanisms can be different but with minor exceptions no valley parallel normal faulting is predicted. No reasonable regional strain field can be found that predicts valley parallel normal faulting.

We verify that a combination of localised and distributed deformations can explain the main features of deformation observed in the region of the Dead Sea and in particular the absence of large valley parallel normal faults. Such faulting however has been observed to occur under different boundary conditions in another tectonic context. Fig. 8 gives the example of the Kunlun fault in Tibet along which slip was partitioned between a pure normal and a pure strike-slip fault. Fig. 8a shows the picture of the cumulative normal fault scarp that is parallel to, and 2 km from the Kunlun strike-slip fault. Surface rupture associated with the Kokoxili earthquake, 2001 can be seen along the normal fault scarp and strike-slip rupture in the foreground (Klinger et al., 2005). Fig. 8b shows the slip directions predicted for a model of oblique faulting at depth. The reader can find more detailed modelling in King et al. (2005). The complete partitioning into two distinct faults results from a locally generated strain field being superimposed on a regional strain field with a different extension direction. To create a similar effect for the Jordan valleys would require a regional extension direction of between 95° and 145°E. There is no evidence that such a field exists and ample evidence for an extension axis of about 50°E (Hofstetter et al., 2007).

7. Estimating the relative proportions of localised and distributed deformation

We have shown that the topography observed in the region of the Dead Sea valleys is well reproduced by applying a Burger's vector having a component ($u=1$) of strike-slip, ($v=0.2$) of opening and ($w=0.03$) of dip-slip on two main fault elements with an angle of $\alpha=11.5°$ between them (Fig. 9). The choice of these values corresponds to the best fit and has been discussed earlier. The deformation is proportional to the Burgers vector with the relative contribution of each component being equal to

$$\text{strike} - \text{slip} = 1.00 \times 100 / 1.23 = 81.3\%$$

$$\text{opening} = 0.20 \times 100 / 1.23 = 16.3\%$$

$$\text{dip} - \text{slip} = 0.03 \times 100 / 1.23 = 2.4\%$$

If we assume to a first approximation that the dislocations are semi-infinite in length, the two Somigliana elements can be described using three line (Volterra) dislocations. The strike-slip contribution is divided into strike-slip deformation on the two dislocations parallel to the surface (L1 and L2) and distributed deformation caused by the change in strike. The latter results from the vertical edge dislocation H that has a Burger's vector equal to $2u \sin(\alpha/2) = 0.2\,u$ and induces the uplift and subsidence shown in Fig. 6d and also shear in the horizontal plane (not shown). Assuming to a first approximation that the dislocations are semi-infinite, 20% of the 81.3% i.e. 16.3% of the strike-

slip contribution, associated with the change of strike, is therefore distributed. In summary,

Localised strike-slip	~65%
Distributed deformation associated with change of strike	~16%
Distributed deformation associated with opening	~16%
Distributed deformation associated with dip-slip	~2%

Therefore, for the parameters we have adopted, about 65% of the total deformation, corresponds to the strike-slip component much of which can be accommodated by through going strike slip faults within the valley. The remainder, about 35%, cannot localise and must be accommodated by distributed deformation. For a smaller opening rate, the agreement between the observed and predicted topography (Fig. 5c) is less convincing but we can nevertheless explore its influence on these ratios. Adopting a value five times smaller for the opening component while keeping the same strike-slip and dip-slip components would lead to a relative increase in the strike-slip contribution to the deformation. Overall, about 75% of the deformation would then be able to localise but 25% at least would still have to remain distributed.

Although exact values depend upon our assumptions about opening rates, it is reasonable to propose the larger proportion of the deformation, which is strike-slip can be accommodated by

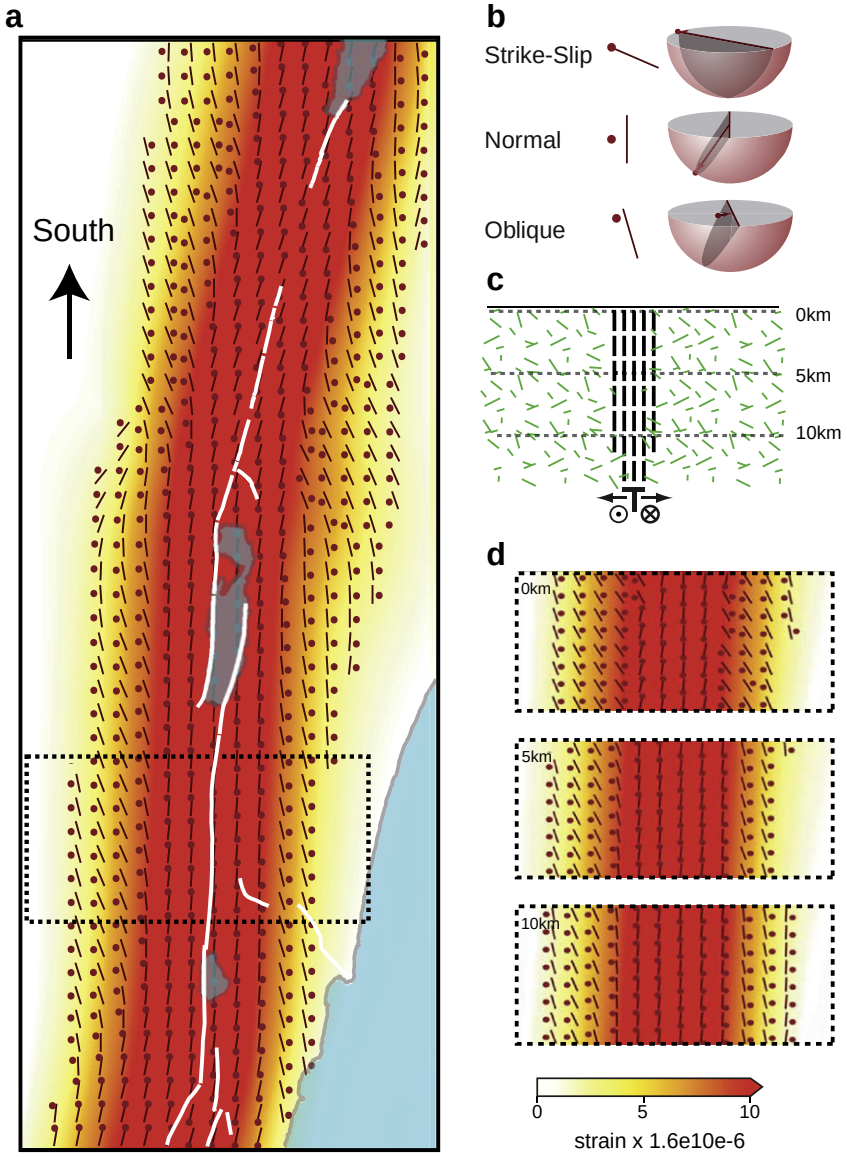

Fig. 7. Predicted slip directions in the Dead Sea region. A regional vertical strain of $-1.6\,10^{-6}$ and a horizontal strain of $3.2\,10^{-6}$ at −40°E and of 0.0 at 50°W are applied. a) Shows predicted directions for strike-slip, normal and oblique faults with left-lateral components at a depth of 5 km. The shading indicates strain (= Geometric moment per unit volume). Note that only one of two possible dip directions is shown for normal faults. An inset, bottom right shows the scale. Note that across the width of the rift the colour scale is saturated. Only the strike-slip mechanisms near the centre of the rift allow the creation of long kinematically stable faults parallel to the valley axis. These are consistent with the main active strike-slip faults. Many mechanisms on the flanks are normal with an extension direction ~50° E. Others have oblique mechanisms with varying ratios of normal to strike-slip components. Normal faulting parallel to the valley is not predicted. A change in the distribution of dislocation sources used to model deformation can slightly change the predicted slip directions but won't affect our main conclusions — flank deformation cannot localise on single through-going faults. b) Shows the interpretation of the mechanisms shown in b), d) and e). c) Shows a schematic cross-section indicating where strike-slip faulting can form (vertical lines) and where faulting cannot localise (green hatching) and indicates the depths at which a) and d) are calculated. d) Shows predicted directions for different depths. Strike-slip mechanisms are predicted at all depth along the valley axis. Away from the axis many mechanisms become oblique and are different at different depths. Normal faults parallel to the valley cannot develop. Since the predicted mechanisms are not kinematically stable other faulting mechanisms must develop resulting in a process zone of distributed deformation that creates the observed form of the valley. (For interpretation of the references to colour in this figure legend, the reader is referred to the web version of this article.)

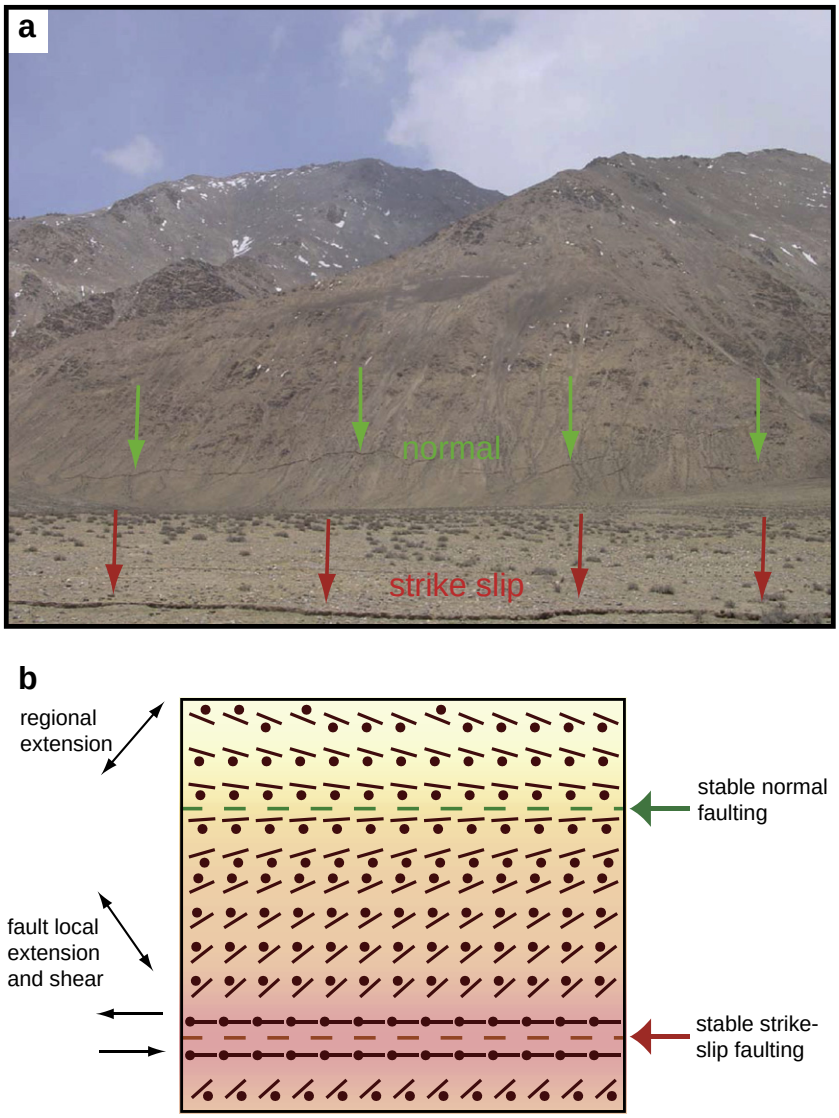

Fig. 8. Slip partitioning in the 2001 Kokoxili earthquake. a) A view showing (parts of the) strike-slip surface breaks in the foreground and normal slip surface breaks along the escarpment in the background. The strike-slip breaks followed the well-established trace of the Kunlun fault and the normal breaks were associated with a well-established normal fault associated with triangular facets and wine glass valleys. b) A model showing local extension in the region of the strike slip faulting and regional extension away from it. These have different orientations creating a zone where stable normal faulting can occur. For greater detail see King et al., 2005.

kinematically stable strike slip faults while a smaller proportion cannot result in kinematically stable faulting and has to be accommodated by distributed deformation.

8. Discussion

In this paper, we describe deformation in the lithosphere considering it to behave as a strain weakening elasto-plastic material. This approach is different from modelling the lithosphere using an assemblage of rigid blocks or as a fluid. Such models are built by making extreme assumptions about the rheology. Within these frameworks, the co-occurrence of localised and distributed deformation in the lithosphere has been difficult to explain. The use of more and more complicated rheologies, taking into account the dependency of viscosity on various parameters such as temperature, pressure, fluid environment, grain size etc. has not led to any significant improvement. The difficulty for such modelling arises for two reasons. First, because three dimensional calculations with realist kinematic boundary conditions are unmanageable with existing computing capacity and probably for computing capacity in the foreseeable future and second because even at the lab scale, the dependency of the deformation of strain weakening elasto-plastic materials on the geometry and kinematics of the boundary conditions are not understood.

On the basis of simple geometric and kinematic considerations however we show how in strain-softening materials such as the lithosphere, most boundary conditions induce a complicated strain field that can only be released by a combination of localised and distributed deformation. The latter occurs in process zones that are located at complexities on the fault systems along which deformation localises.

Considering that the lithosphere behaves as a strain-softening material, we produce a model of the deformation in the Dead Sea region that is consistent with creating features of the morphology observed today. We use a combination of dislocations to reproduce the deformation field. The only assumption made using this approach is that the medium is continuous and responds linearly to each increment of strain. The only material parameter that is required is Poisson's ratio. The resulting model (Fig. 5c) reproduces major features of the observed topography much better than using other

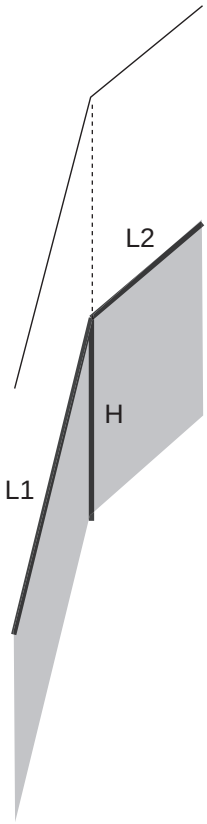

Fig. 9. Line dislocations used for quantifying the ratio between distributed and localised deformation, discussed in the text.

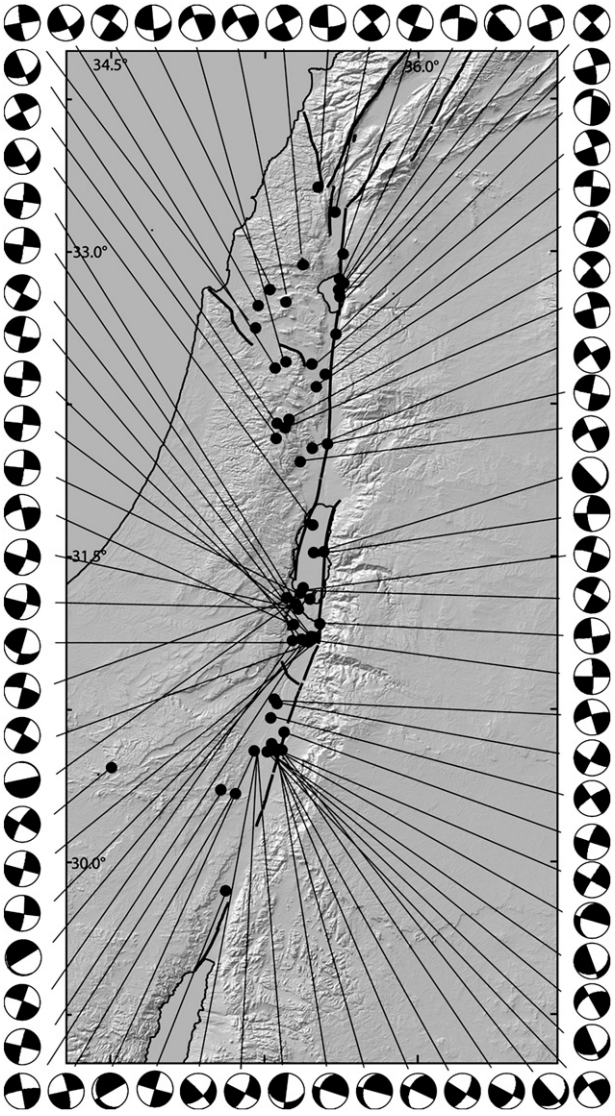

Fig. 10. Focal mechanisms along the Dead Sea valleys, modified from Hofstetter et al. (2007). The multiple orientations of the fault planes are consistent with resulting from distributed brittle deformation. See also more detailed maps in the same paper. Similar multiple mechanism faulting and associated strain relief for northern California is discussed by Amelung and King (1997a,b).

modelling approaches. It provides, in particular, an explanation for the relatively high elevation of the Araba compared to the Jordan valley, an observation hitherto unexplained.

Armed with the deformation model we consider the implications of the crustal rocks exhibiting a strain-softening behaviour. In such materials deformation localises to form faults or shear zones where slip directions are collinear on long distances. Deformation occurs in a distributed manner elsewhere. The model predicts that deformation can localise along strike-slip faults within the valleys but must remain distributed elsewhere, occurring on small faults with various orientation. This is consistent with the observation of large-scale strike-slip faulting within the valleys and the absence of major normal faults outlining the valley sides. The multi-scale multi-direction faulting predicted for the distributed deformation is strongly supported by the highly variable focal mechanisms for small earthquakes along the valleys (Fig. 10, Hofstetter et al., 2007).

There are numerous other examples of the distributed deformation that we describe here. They include the northern and southern parts of Death Valley and Fish lake valley, which like the Dead Sea valleys exhibit strike-slip faults but no significant normal faults; yet both strike-slip and extension are active. They are very similar in form to the Dead Sea valleys. The relation between motion in the southern East California Shear Zone (Imperial, Panamint and Death Valleys) and deformation in the Eastern Mojave also requires distributed deformation. In Greece, the North Anatolian fault in the Aegean is clearly kinematically related to the Gulf of Corinth (e.g. Armijo et al., 1996), but the connection must be accommodated by distributed deformation since no simple connecting structures can be found.

On theoretical grounds, it has been proposed that process zones should be stronger than established faults (Cowie and Scholz, 1992), but quantitative values could not be assigned. Although commonly considered to be weak the level of shear stress along major strike-slip faults has been a controversial topic. The stress-heat flow paradox of the San Andreas fault has largely fuelled the debate (Brune et al., 1969; Lachenbruch and Sass, 1980; Scholz, 2000; Scholz, 2006; Zoback et al., 1987). The lack of a significant heat-flow anomaly along the fault suggests a low level of shear stress and argues against shear heating on the fault plane as being an important heating mechanism. Interpretation of stress orientation data has proved to be controversial, but nonetheless has led many to conclude that major faults were very weak (Townend and Zoback, 2004, Zoback et al., 1987). Others have concluded that they were stronger (Miller, 1998; Scholz, 2000) although not as strong as frictional coefficients measured in laboratory experiments would suggest (Byerlee, 1978). The idea of weak faults is supported by various publications, among which that of Lavier et al. (2000) who show that significant weakening is required in order to create very large offset faults in continental rift settings. Processes of dynamical weakening (thermal pressurisation of pore fluid, flash heating at microasperities for instance) have been invoked to explain the weakness of a well-localised fault plane during a rupture propagation (e.g. Rice, 2006; Sibson, 1977).

John Suppe (2007) has recently shown directly that the strength of the distributed deformation of an accreting wedge where deformation is distributed is ten times greater than that of the underlying localised detachment fault. This is a robust measurement of the relative strengths. Furthermore it is at the scale of the problem that we are considering and does not require extrapolation of laboratory scale data to scales 10^7 times greater. If the same relation applies between the percentage of strike-slip and of distributed deformation calculated for the Dead Sea valleys then the strike-slip motion will contribute at most to a quarter of the resistance to motion for this part of the plate boundary. Distributed deformation associated with geometric complexities will therefore provide most of the resistance to motion along the plate boundary and not faults themselves. It then follows that process zones of distributed deformation should be the locus of most energy dissipation, much of which will be converted into heat.

9. Conclusions

Deformation in the lithosphere has often been thought to depend only on pressure, temperature, fluid environment, material composition and microstructure (e.g. Kohlstedt et al., 1995). The importance of the geometric and kinematic evolution of boundary conditions in controlling the deformation style has largely been ignored. In strain-softening materials however, it seems to control the deformation style causing some deformation to localise along simple shear directions and some deformation to remain distributed in process zones where kinematic incompatibility prevents localisation to occur over long distances. This geometric and kinematic control on deformation is observed from scales of centimetres or less to tens of kilometres or more. We explore the implications of modelling the lithosphere, where both localised and distributed deformations occur, as a strain-softening material. To that end, we determine the deformation field associated with the creation of the Dead Sea valleys. Our kinematic model can demonstrably explain the creation of the major features of today's topography. It allows us to quantify the distribution between localised and distributed deformations and to estimate the stress levels associated with each contribution. We find that although only 35% of the deformation is distributed, it provides 3 times more resistance to motion on the Levant boundary than strike-slip motion. It is important to underline that this estimate of the distribution and level of stresses at plate boundaries only relies on kinematics and not on the extrapolation of small-scale rheological laws, which behaviours are still poorly understood. Our approach therefore provides an important alternative method for improving our understanding of lithosphere deformation. Although our case study concerns the crust it can be applied to the whole lithosphere if it is considered to behave in a similar way. We suggest that the resistance to motion results mainly from distributed deformation in process zones associated with geometric complexities on fault systems and not from faults themselves. These process zones must therefore be the locus of most energy dissipation, most of which must be converted into heat. This has implications for our understanding of the origin of metamorphism and magma genesis in the lithosphere.

Acknowledgements

The authors would like to thank Charles Sammis and Rick Ryerson for discussion and criticism of earlier versions of this work. Two anonymous reviewers have helped to improve the manuscript. GK would like to thank the Hebrew University of Jerusalem for a generous 3 month fellowship during which he gained a greater understanding of the diverse opinions of the evolution of Levant plate boundary. The project has also received support from the “Disperse” project of the European Science Foundation and the “Galilee Project” a charity registered in the UK. This is IPGP contribution number 3175.

Appendix A. Supplementary data

Supplementary data to this article can be found online at doi:10.1016/j.epsl.2011.05.044.

References

Amelung, F., King, G.C.P., 1997a. Large scale tectonic deformation inferred from small earthquakes. Nature 386, 702–705.
Amelung, F., King, G.C.P., 1997b. Earthquake scaling laws for creeping and non-creeping faults. EPSL 24 (5), 507–510.
Amit, R., Zilberman, E., Enzel, Y., Porat, N., 2002. Paleoseismic evidence for time dependency of seismic response on a fault system in the southern Araba valley, Dead Sea rift, Israel. Geol. Soc. Am. Bull. 114, 192–206.
Armijo, R., Meyer, B., King, G.C.P., Rigo, A., Papanastassiou, D., 1996. Quaternary evolution of the Corinth Rift and its implication for the late Cenozoic evolution of the Aegean. Geophys. J. Int. 126 (1), 11.
Armijo, R., Flerit, F., King, G.C.P., Meyer, B., 2003. Linear elastic fracture mechanics explains the past and present evolution of the Aegean. Earth Planet. Sci. Lett. 217, 85–95.
Bilham, R.G., King, G.C.P., 1989. The morphology of strike-slip faults: examples from the San Andreas fault, California. J. Geophys. Res. 94 (B8), 10.
Bowman, D., King, G.C.P., Tapponnier, P., 2003. Slip partitioning by elasto-plastic propagation of oblique slip at depth. Science 300, 1121.
Brune, J.N., Henyey, T.L., Roy, R.F., 1969. Heat flow, stress, and rate of slip along the San Andreas Fault, California. J. Geophys. Res. 74, 3821.
Byerlee, J.D., 1978. Friction of rocks. Pure Appl. Geophys. 116, 615.
Cowie, P.A., Scholz, C.H., 1992. Physical explanation for the displacement-length relationship of faults using a post-yield fracture mechanics model. J. Struct. Geol. 14 (10), 1133.
Crouch, S.L., Starfield, A.M., 1983. Boundary Element Methods in Solid Mechanics. Allen Unwin, Concord, MA.
De Sitter, L.U., 1964. Structural Geology. McGraw-Hill, New York, San Francisco, Toronto, London.
Eshelby, J.D., 1973. Dislocation theory for geophysical applications. Phil. Trans. R. Soc. Lond. A. 274, 331–338.
Flerit, F., Armijo, R., King, G.C.P., Meyer, B., Barka, A., 2003. Slip partitioning in the Sea of Marmara pull-apart determined from GPS velocity vectors. Geophys. J. Int. 154, 1–7.
Flerit, F., Armijo, R., King, G.C.P., Meyer, B., 2004. The mechanical interaction between the propagating North Anatolian Fault and the back-arc extension in the Aegean. Earth Planet. Sci. Lett. 224, 347–362.
Freund, R., Zak, I., Garfunkel, Z., 1968. Age and rate of the sinistral movement along the Dead Sea rift. Nature 220, 253–255.
Garfunkel, Z., 1981. Internal structure of the Dead Sea leaky transform (Rift) in relation to plate kinematics. Tectonophyics 80, 81–108.
Garfunkel, Z., 1997. The history and formation of the Dead Sea basin in The Dead Sea, the lake and its setting. In: Niemi, T., Ben-Avraham, Z., Gat, J. (Eds.), Oxford Monographs on Geology and Geophysics #36. Oxford Univ. Press, New York, USA.
Garfunkel, Z., Zak, I., Freund, R., 1981. Active faulting in the Dead Sea rift. Tectonophysics 80, 1–26.
Henstock, T.J., Levander, A., Hole, J.A., 1997. Deformation in the lower crust of the San Andreas fault system in Northern California. Science 278, 650–653.
Hofstetter, R., Klinger, Y., Amrat, A.-O., Rivera, L., Dorbath, L., 2007. Stress tensor and focal mechanisms along the Dead Sea fault and related structural elements based on seismological data. Tectonophysics 429, 165–181.
Hubert-Ferrari, A., King, G.C.P., Manighetti, I., Armijo, R., Meyer, B., Tapponnier, P., 2003. Long-term elasticity in the continental lithosphere; modelling the Aden Ridge propagation and the Anatolian extrusion process. Geophys. J. Int. 153, 111–132.
Hubert-Ferrari, A., King, G.C.P., Van der Woerd, J., Villa, I., Altunel, E., Armijo, R., 2009. Long-term evolution of the North Anatolian Fault: new constraints from its eastern termination. Geol. Soc. London Spec. Pub. 311 (1), 133.
Jaeger, J.C., Cook, N.G.W., Zimmerman, R.W., 2007. Fundamentals of Rock Mechanics, 4th Edition. John Wiley & Sons.
King, G.C.P., 1983. The accommodation of large strains in the upper lithosphere of the earth and other solids by self-similar fault system: the geometrical origin of b-value. Pure Appl. Geophys. 121, 761.
King, G.C.P., 1986. Speculations on the geometry of the initiation and termination processes of earthquake rupture and its relation to morphology and geological structure. Pure Appl. Geophys. 124, 567.
King, G.C.P., 2007. Fault interaction, earthquake stress changes and the evolution of seismicity. In: Schubert, G. (Ed.), Treatise on Geophysics, Volume 4. Elsevier Ltd., Oxford, pp. 225–256.
King, G.C.P., Brewer, J., 1983. Fault related folding near the Wind River thrust, Wyoming, U.S.A. Nature 306, 147.
King, G.C.P., Nabelek, J., 1985. The role of bends in faults in the initiation and termination of earthquake rupture: implications for earthquake prediction. Science 228, 986–987.
King, G.C.P., Yielding, G., 1984. The evolution of a thrust fault system: processes of rupture initiation, propagation and termination in the 1980 El Asnam (Algeria) earthquake. Geophys. J. Royal Astr. Soc. 77, 605.
King, G.C.P., Klinger, Y., Bowman, D., Tapponnier, P., 2005. Slip-partitioned surface breaks for the Mw 7.8, 2001, Kokoxili earthquake China. Bull. Seismol. Soc. Am. 95, 731.

Klinger, Y., 2010. Relation between continental strike-slip earthquake segmentation and thickness of the crust. J. Geophys. Res. 115, B07306. doi:10.1029/2009JB006550.
Klinger, Y., Avouac, J.P., Dorbath, L., Abou Karaki, N., Tisnerat, N., 2000. Seismic behaviour of the Dead Sea fault along Araba valley, Jordan. Geophys. J. Int. 142, 769–782.
Klinger, Y., Xu, X., Tapponnier, P., Van der Woerd, J., Laserre, C., King, G., 2005. High-resolution satellite imagery mapping of the surface rupture and slip distribution of the Mw ~7.8, November 14, 2001 Kokoxili earthquake (Kunlun fault, Northern Tibet, China). Bull. Seismol. Soc. Am. 95 (5), 1970–1987.
Klinger, Y., Michel, R., King, G.C.P., 2006. Evidence for an earthquake barrier model from Mw7.8 Kokoxili (Tibet) earthquake slip-distribution. Earth Planet. Sci. Lett. 242, 354.
Kohlstedt, D.L., Evans, B., Mackwell, S.J., 1995. Strength of the lithosphere: constraints imposed by laboratory experiments. J. Geophys. Res. 100 (B9), 17587.
Lachenbruch, A.H., Sass, J.H., 1980. Heat flow and energetics of the San Andreas fault zone. J. Geophys. Res. 85, 6185.
Lavier, L.L., Buck, W.R., Poliakov, A.N.B., 2000. Factors controlling normal fault offset in an ideal brittle layer. J. Geophys. Res. 105 (B10), 23341–23442.
Leloup, P.H., Kienast, J.R., 1993. High temperature metamorphism in a major tertiary ductile continental strike-slip shear zone: the Ailao Shan-Red River (P.R.C.). Earth Planet. Sci. Lett. 118, 213–234.
Little, T.A., Holcombe, R.J., Ilg, B.R., 2002. Kinematics of oblique collision and ramping inferred from microstructures and strain in middle crustal rocks, central Southern Alps, New Zealand. J. Struct. Geol. 24, 219–239.
Manighetti, I., King, G.C.P., Sammis, C., 2004. The role of off-fault damage in the evolution of normal faults. Earth Planet. Sci. Lett. 217, 339–408.
McClintock, F.A., 1971. Plasticity aspects of fracture in fracture. An advanced treatise. In: Liebowitz, H. (Ed.), Engineering Fundamentals and Environment Effects, Vol. III. Academic Press, New York. 1971.
Meade, B.J., Hager, B.H., 2005. Block models of crustal motion in southern California constrained by GPS measurements. J. Geophys. Res. 110, B03403. doi:10.1029/2004JB003209.
Meade, B.J., Hager, B.H., McClusky, S., Reilinger, R., Ergintav, S., Lenk, O., Barka, A., Ozener, H., 2002. Estimates of seismic potential in the Marmara Sea Region from block models of secular deformation constrained by global positioning system measurements. Bull. Seismol. Soc. Am. 92 (1), 208.
Meyer, B., Tapponnier, P., Bourjot, L., Métivier, F., Gaudemer, Y., Peltzer, G., Shunmin, G., Zhitai, C., 1998. Mechanisms of active crustal thickening in Gansu-Qinghai, and oblique, strike-slip controlled, northeastward growth of the Tibet plateau. Geophys. J. Int. 135 (1), 1.
Miller, D.D., 1998. Distributed shear, rotation, and partitioned strain along the San Andreas Fault, Central California. Geology 26 (10), 867.
Molnar, P., Dayem, K.E., 2010. Major intracontinental strike-slip faults and contrasts in lithospheric strength. Geosphere 6 (4), 444–467. doi:10.1130/GES00519.1. August.
Morgan, W.J., McKenzie, D.P., 1969. Evolution of triple junctions. Nature 224, 125–133. doi:10.1038/224125a0.
Nabarro, F.R.N., 1967. Theory of Crystal Dislocations. Dover, UK. October.
Nyst, M., Thatcher, W., 2003. New constraints on the active tectonic deformation of the Aegean. J. Geophys. Res. 109 (B11), B11406. doi:10.1029/2003JB002830.
Okada, Y., 1985. Surface deformation to shear and tensile faults in a half space. Bull. Seismol. Soc. Am. 75, 1135–1154.
Peltzer, G., Tapponnier, P., 1988. Formation and evolution of strike-slip faults, rifts, and basins during the India-Asia collision: an experimental approach. J. Geophys. Res. 93 (B12), 15085.
Reches, Z., 1983. Faulting of rocks in three dimensional strain fields II. Theoretical analysis. Tectonophysics 95, 133.
Reches, Z., Dieterich, J.H., 1983. Faulting of rocks in three dimensional strain fields, I. Failure of rocks in polyaxial, servo-control experiments. Tectonophysics 95 (1–2), 111.
Regenaeur-Lieb, K., Rosenbaum, G., Weinberg, R.F., 2008. Strain localization and weakening of the lithosphere during extension. Tectonophysics 458 (1–4), 96–104.
Rice, J.R., 2006. Heating and weakening of faults during earthquake slip. J. Geophys. Res. 111 (B05311). doi:10.1029/2005JB004006.
Sagy, A., Reches, Z., Agnon, A., 2003. Hierarchic three-dimensional structure and slip partitioning in the western Dead Sea pull-apart. Tectonics 22 (1), 1004.
Scholz, C.H., 2000. Evidence for a strong San Andreas fault. Geology 28 (2), 163.
Scholz, C.H., 2006. The strength of the San Andreas fault: a critical analysis. Geophys. Monograph 170, 301.
Sibson, R.H., 1977. Kinetic shear resistance, fluid pressures and radiation efficiency during seismic faulting. Pageoph 115.
Stein, R., King, G.C.P., Rundle, J., 1988. The growth of geological structures by repeated earthquakes: 2 Field examples of continental dip-slip faults. J. Geophys. Res. 93 (B11), 13319–13331.
Suppe, J., 1984. Principles of Structural Geology. Prentice Hall, New York. pp 155.
Suppe, J., 2007. Absolute fault and crustal strength from wedge tapers. Geology 35 (12), 1127.
Tapponnier, P., Zhiqin, X., Roger, F., Meyer, B., Arnaud, N., Wittlinger, G., Jingsui, Y., 2001. Oblique stepwise rise and growth of the Tibet plateau. Science 294 (5547), 1671.
Titus, S.J., Medaris, L.G., Wang, H.F., Tiko, B., 2007. Continuation of the San Andreas fault system into the upper mantle: evidence from spinel peridotite xenoliths in the Coyote Lake basalt, central California. Tectonophysics 429 (1–2), 1.
Townend, J., Zoback, M.D., 2004. Regional tectonic stress near the San Andreas fault in central and southern California. Geophys. Res. Lett. 31 (L15S11).
Wittlinger, G., Tapponnier, P., Poupinet, G., Mei, J., Danian, S., Herquel, G., Masson, F., 1998. Tomographic evidence for localized lithospheric shear along the Altyn Tagh fault. Science 282 (5386), 74.
Wu, J.E., McClay, K., Whitehouse, P., Dooley, T., 2009. 4D analogue modelling of transtensional pull-apart basins. Mar. Pet. Geol. 26 (8), 1608–1623.
Zhu, L., 2000. Crustal structure across the San Andreas Fault, southern California from teleseismic converted waves. Earth Planet. Sci. Lett. 179 (1), 183.
Zoback, M.D., Zoback, M.L., Mount, V.S., Suppe, J., Eaton, J.P., Healy, J.H., Oppenheimer, D., Reasenberg, P., Jones, L., Raleigh, C.B., et al., 1987. New evidence on the state of stress of the San Andreas fault system. Science 238 (4830), 1105.